

STOICHIOMETRY AIR–CH₄ MIXTURE: COMPOSITION, THERMODYNAMIC PROPERTIES AND TRANSPORT COEFFICIENTS

A. HARRY SOLO*, M. BENMOUFFOK, P. FRETON, J.J. GONZALEZ

Laplace, UMR 5213 CNRS-UPS-INP, Université Paul Sabatier 118 route de Narbonne, bat3R2, 31062 Toulouse Cedex France

* andriniaina.harry@laplace-univ.tlse.fr

Abstract. This work is related to the determination of the local thermodynamic equilibrium (LTE) data of 90.5% air and 9.5% CH₄ mixture. The results of chemical composition, thermodynamic properties and transport coefficients are presented for temperatures (300 K to 30 kK) and pressure (1 and 10 bars) or mass density (0.1481 and 1.111 kg.m⁻³). The chemical composition is determined using the mass action law. Input data come from the NIST and JANAF sites. For pressure equation, Debye-Huckel's first order and virial's second order corrections are used in the equation system to take into account the different particle interactions. For the considered mixture (90.5% air and 9.5% CH₄) the properties are compared to those of pure air.

Keywords: air–CH₄, plasma composition, constant pressure, constant mass density, thermodynamic properties, transports coefficients..

1. Introduction

The CH₄–air gas mixture is generally used in the ignition studies of thermal engines [1–3]. The used mixture proportions change according to the literature works, and are sometimes subject of parametric studies [1, 3]. However, it is difficult to find the data for the desired conditions (temperature range, pressure, or mixture proportions). So mixing laws are sometimes used, whereas they are inappropriate for reactive gases. Other authors consider the mole proportion of methane in the mixture to be small (5-10%) and use air data [2, 4]. These assumptions may lead to erroneous results, or at least far from real behavior. Our goal in this paper is to determine a database for a mixture of 90.5% air and 9.5% CH₄ in order to be able to implement in the future a plasma modelling after the spark phase of an ignition process. We present our calculation method and the equations system under the hypothesis of local thermodynamic equilibrium (LTE). The results of the air-methane mixture will be compared with those of air, and with results from the literature.

2. Theory

2.1. Partition function

The determination of the data needs generally the internal partition functions Q_{int} of species and their derivatives. They are calculated from equations (1) or (8). The input parameters used come from the NIST [5] and JANAF [6] sites. Using atomic levels from the NIST database, the sets are not complete as some levels are missing. In this case, the NIST dataset should be completed before the calculation of the partition function. Several theoretical approaches allow to complete the database set [7–9]. For example,

the semi-empirical procedure from Ritz-Rydberg [10], applying a simplified formula to available, experimental or calculated, electronic levels, allows to complete, interpolating and/or extrapolating, the level series. Two adjustable parameters are calculated sometime by solving a system of two equations from adjacent levels. In our case the NIST database was not completed. However a good agreement is obtained with Capitelli et al [10] in case of an air plasma. These equations are solved for a temperature step of 1 K and the derivatives passed in a spline to avoid oscillations in thermodynamic properties as well as transport coefficients.

□ Atomic Species

$$Q_{\text{int}}(T) = \sum_i^{i_{\text{max}}} g_i \exp\left(-\frac{E_i}{k_B T}\right) \quad (1)$$

with g_i the statistical weight given by $g_i = 2J + 1$, where J is the quantum number of angular moment, k_B the Boltzmann constant, T the temperature, E_i the energy of electronic level, and i_{max} the limit of the summation such as:

$$E_{i_{\text{max}}} \leq E_{\text{ion}} - \Delta E \quad (2)$$

E_{ion} is the ionization energy and ΔE the lowering of ionization potential [11]. A suitable cut-off is necessary to prevent the divergence of electronic partition functions. Mainly, three criteria can be used as explained by Capitelli et al [10]: (a) The ground state method. (b) The Debye-Hückel cutoff criteria (Griem and Margenau and Lewis) (c) The Fermi criterion. Some works were devoted to this specific point as the study of Colonna et al [9]. In our tool we have used the Griem criterion.

Laws	Equations
Mass action	$\prod_{i=1}^N n_i^{v_i} = \prod_{i=1}^N Q_{\text{tot},i}^{v_i} \quad (3)$
Conservation of atomic nucleus	$\epsilon_j \sum_i^N n_i C_{i,k} = \epsilon_k \sum_i^N n_i C_{i,j} \quad (4)$
Conservation of electrical neutrality	$\sum_i^N Z_i n_i = 0 \quad (5)$
Dalton	$P = \sum_i^N n_i k_B T + \Delta P_{\text{Debye}} + \Delta P_{\text{virial}} \quad (6)$
Conservation of mass density	$\rho = \sum_i^N n_i m_i \quad (7)$

Table 1. Basis equations used to determine the chemical composition.

□ Molecular Species

$$Q_{\text{int}}(T) = \frac{P_r}{k_B T} \left(\frac{h^2}{2\pi m k_B T} \right)^{\frac{3}{2}} \exp \left[\frac{1}{N_a k_B} \left(\frac{[H(0) - H(T_r)]_{\text{JANAF}}}{T} - \left[\frac{G - H(T_r)}{T} \right]_{\text{JANAF}} \right) \right] \quad (8)$$

with P_r and T_r respectively the pressure and reference temperature in the JANAF table [6], h the Planck constant, m the mass of the species, N_a the Avogadro number, $[H(0) - H(T_r)]$ the enthalpy evaluated at zero kelvin, and $[G - H(T_r)]/T$ the temperature-dependent Gibbs energy. The internal partition functions of molecules are calculated according to the formalism mentioned by Godin et al [12]. This approach is based on the enthalpy evaluated at zero kelvin and on the Gibbs free energy given versus temperature. JANAF tables usually consider only one electronic level of the molecules, and neglects quasi-bound states. These effects can be important at high temperature and pressure [10]. Nevertheless the comparison made with Billoux [13] in case of an air plasma at 100 bars which has used another formalism for the calculation of the partition functions gives similar results. Indeed molecular species can be assumed negligible at high temperature compared to the atoms.

2.2. Chemical composition

The calculation of chemical composition was developed using the mass action law including the chemical base concept [14]. This method allows us to generalize the equations for different types of pure gases and gas mixtures. If calculation is performed at constant pressure, Dalton's law is used with the corrections of Debye-Hückel δP_{Debye} and virial δP_{virial} [11, 15]. Correction needs also to be made for the mass action law. In the equation (3) the correction term is

included in the total expression of the partition function. For a calculation performed at constant density, the mass density equation is used. The basic equations for the determination of chemical composition are summarized in Table 1.

In Table 1, N represents the total number of chemical species, n_i the density of the species i , v_i the stoichiometry coefficients of the reaction, $Q_{\text{tot},i}$ the total partition function by volume, ϵ the atomic proportion of the species j or k , $C_{i,k}$ and $C_{i,j}$ the elements of the composition matrix [11], and Z_i the charge of the species.

2.3. Thermodynamic properties

Knowing the densities of each species, as well as their internal partition functions, the thermodynamic properties can be calculated (such as mass density ρ , enthalpy H or specific heat capacity at constant pressure C_p). These properties are generally presented for a given pressure [15]. Here we will look at internal energy U and specific heat capacity at constant volume C_v . These data are used particularly in variable pressure and constant volume systems. Their equations are illustrated in Table 2 where N_i [in kg^{-1}] is given by $N_i = n_i/\rho$, and E_i^{ref} is the reference energy. All the virial corrections according to Kallmann [16], and Debye-Hückel corrections from Capitelli et al [10] are included in ours developments. More complete correction expressions are given by Capitelli et al [10]. Nevertheless in our work the corrections are limited to the first term (Second virial coefficient) [16]. In equations (9) and (10), ΔU_p and $\Delta C_{v,p}$ refer respectively to the internal energy correction and to the specific heat correction at constant volume.

2.4. Comparison - Validation

In this section we present in order to validate ours developments a comparison of some literature results with ones obtained with our tool. The first comparison is devoted to the plasma composition in the case of an air plasma for a temperature range 300 K to

Thermodynamic properties	Equations
Internal energy	$U = \frac{3}{2} k_B T \sum_i N_i + k_B T^2 \sum_i N_i \cdot \frac{\partial \ln Q_i^{\text{int}}}{\partial T} + \sum_i N_i E_i^{\text{ref}} + \Delta U_p \quad (9)$
Specific heat at constant volume	$C_v = \left(\frac{\partial U}{\partial T} \right)_V + \Delta C_{vp} \quad (10)$

Table 2. Equations to calculate thermodynamic properties.

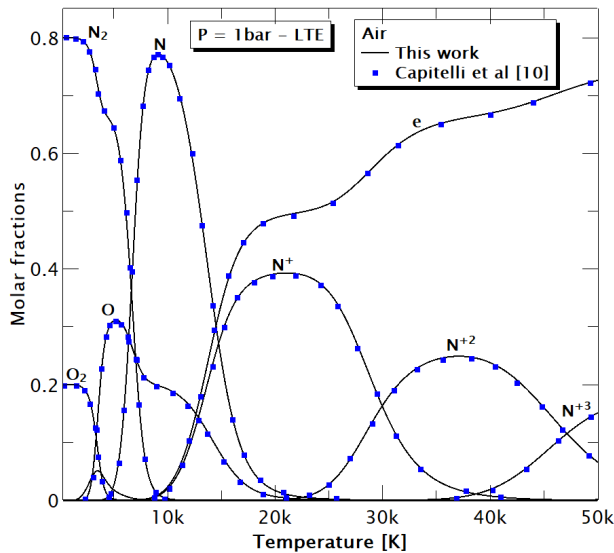


Figure 1. Air composition versus temperature compared with Capitelli et al [10].

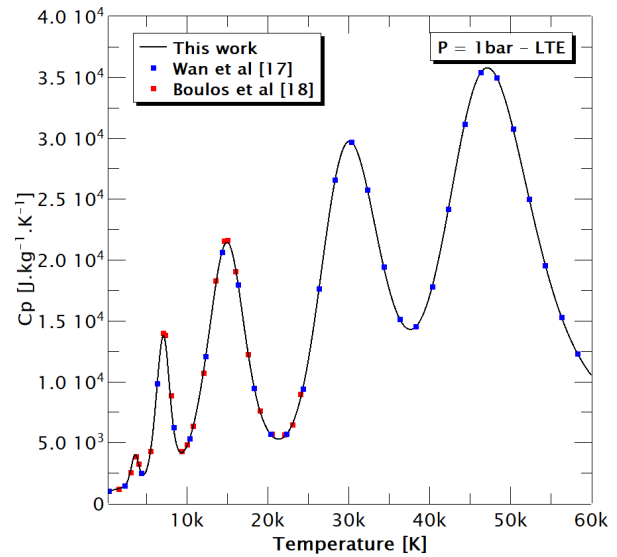


Figure 2. Specific heat of air at 1 bar compared with Wan et al [17] and Boulos et al [18].

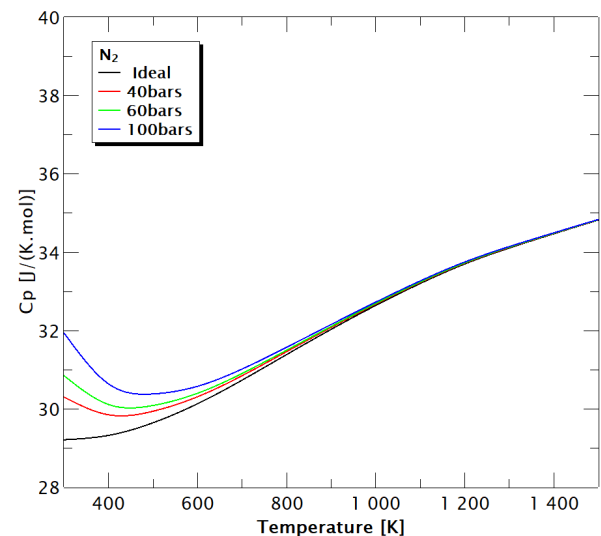
50 kK. The chosen pressure is $P = 1$ bar. The results are compared with them of Capitelli et al [10] and a good agreement is found (in Figure 1). Based on this plasma composition, the thermodynamic properties can be calculated. As an example of validation we compare in Figure 2 the specific heat at constant pressure with the works of Wang et al [17] and Boulos et al [18]. A good agreement is also found. Nevertheless it is interesting to analyse the specific heat at low temperature for higher pressure in order to see the effect of the corrections on the specific heat. Figure 3 presents the evolution of the specific heat for several pressure values compared with the ideal gas in nitrogen case (N_2).

This gas is chosen as it allows a comparison with Capitelli et al [10]. We can observe that the correction effect acts at low temperature increasing with the pressure values. This effect is also encountered by Capitelli et al [10]. However some small differences can be observed with this author due to the fact that in our case the correction is limited to the first order with the second virial coefficient.

2.5. Transport coefficients

The conventional formulations of the literature based on the third approximation order of Chapman-Enskog

method are used for the determination of transport coefficients [19, 20]. The equations to be solved require the knowledge of additional input data that are the collision integrals. In our code, they are calculated in

Figure 3. Comparison of the constant pressure specific heat in N_2 calculated using second virial coefficient from Van der Waals equation with ideal gas calculation according to [16].

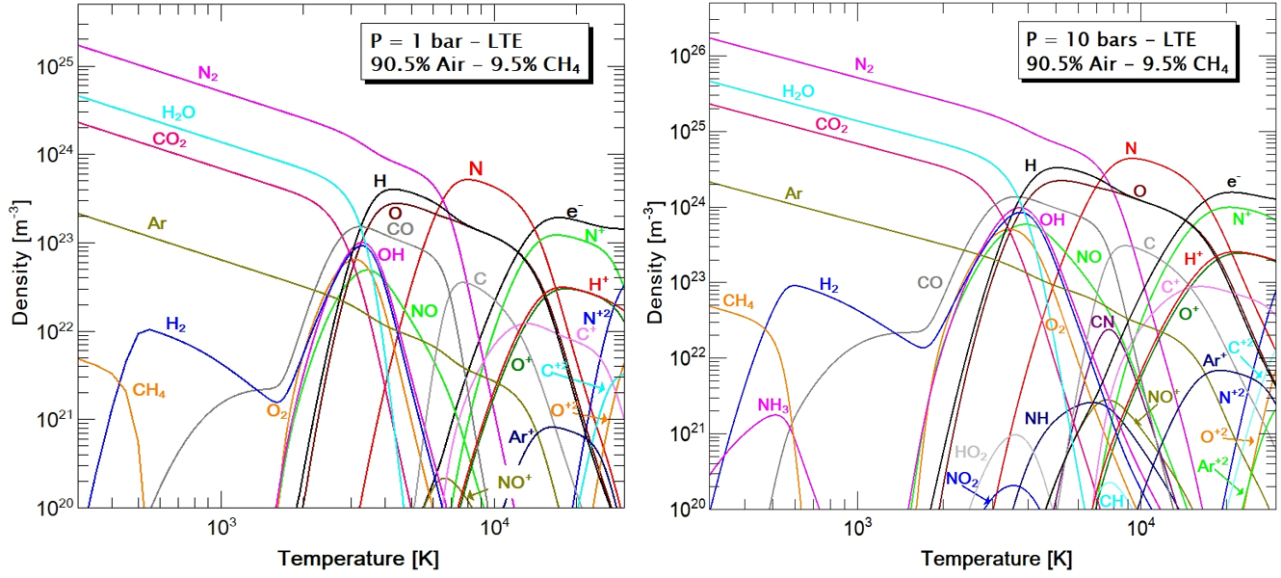


Figure 4. Chemical composition: 90.5% air and 9.5% CH_4 - 1 bar and 10 bars - LTE.

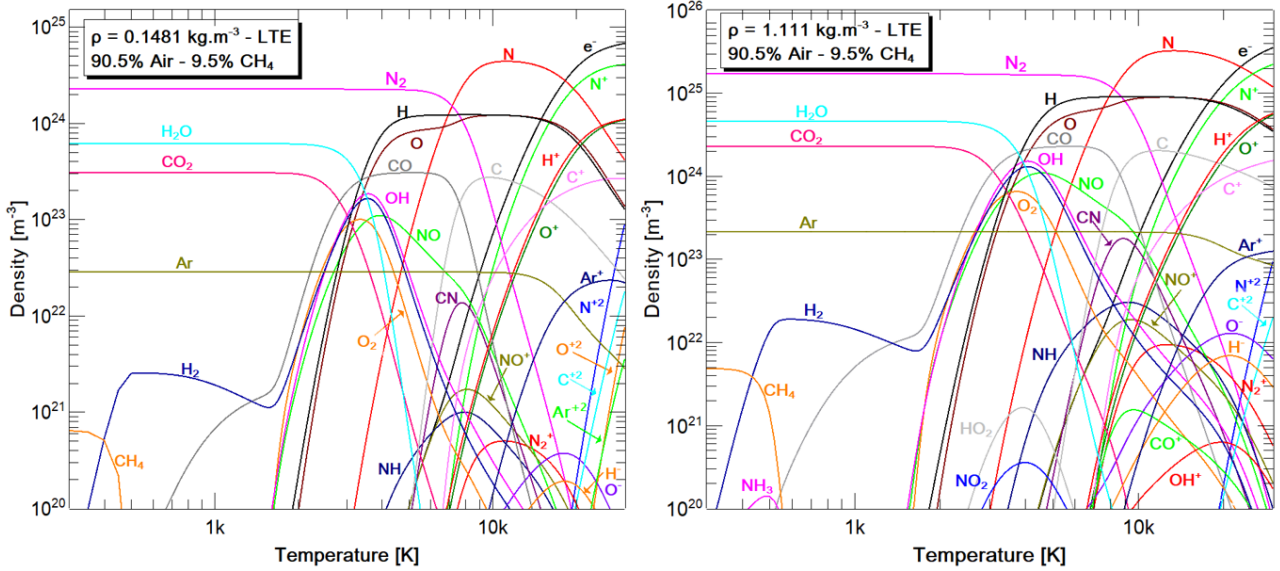


Figure 5. Chemical composition: 90.5% air and 9.5% CH_4 for 0.1481 and 1.111 kg.m^{-3} at LTE.

first approximation from the hard sphere potentials. However, following available data, the appropriate formalism according to the type of collision of the species (Table 3) is considered.

- Case of Charged-Charged interaction: The collision integrals are calculated from Mason et al [21]. The interactions between charged particles are described by Coulomb potential screened by Debye length.
- Case of Neutral-Neutral interaction: Lennard-Jones potential (atoms or molecules). The reduced temperature T_{reduced} is used. This formalism depends on the maximal energy attraction. Tabulated values for the 12-6 Lennard-Jones potential are used [22].
- Case of Neutral-Charged: Electron/Neutral and Charged/Neutral (Input: charge, polarity and T_{reduced}). The parameters used to calculate the

collision integrals come from Capitelli et al [23] for air, and from Baronnet et al [24] as well as Sanon [25, 26] for methane.

In case of neutral-neutral and neutral-ion calculations, we have used cross sections available in the literature (see [27] for example). A comparison of cross-section is of course useful; a comparison with the data used in our article [28] with other authors from literature can be found in the paper from A. D'Angola et al [27].

3. Results and Discussion

We present the results obtained for a mixture of 90.5% air and 9.5% CH_4 for a temperature range from 300 K to 30 kK. 51 species were considered in our calculations: N , N^+ , N^{+2} , N_2 , N_2^+ , NO , NO^+ , N_2O , NH , CN ,

Species(i)/Species(j)	Electron	Neutral	Charged
Electron	Coulomb	Polarity	Coulomb
Neutral	Reciprocity	Lennard Jones	Polarity
Charged	Reciprocity	Reciprocity	Coulomb

Table 3. Used formalism according to the species collision type.

CNO, O, O⁺, O⁺², O⁻, O₂, O₂⁺, O₂⁻, OH, OH⁺, CO₂, HO₂, NO₂, C, C⁺, C⁺², C₂, CO, CO⁺, CH, CHN, CHO, C₂H, C₂H₂, H, H⁺, H⁻, H₂, H₂O, H₂O₂, HNO, NH₂, NH₃, CH₂, CH₃, CH₄, CH₂O, Ar, Ar⁺, Ar⁺², e⁻. A comparison is made between the thermodynamic properties and the transport coefficients of the air-methane mixture and the pure air. For validation, we compare our results with those available in the literature.

3.1. Chemical composition

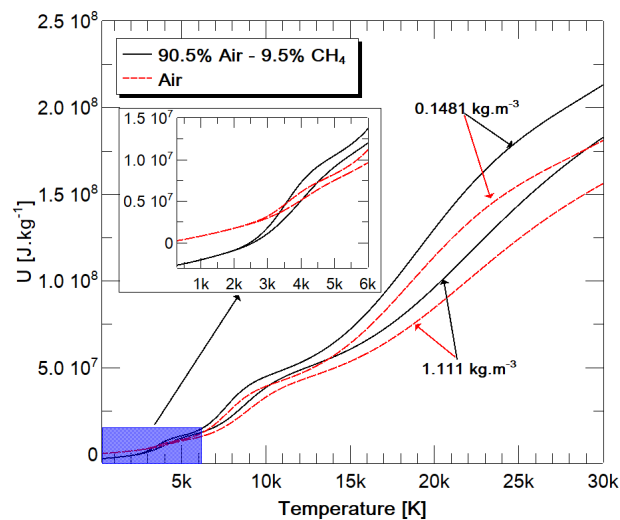
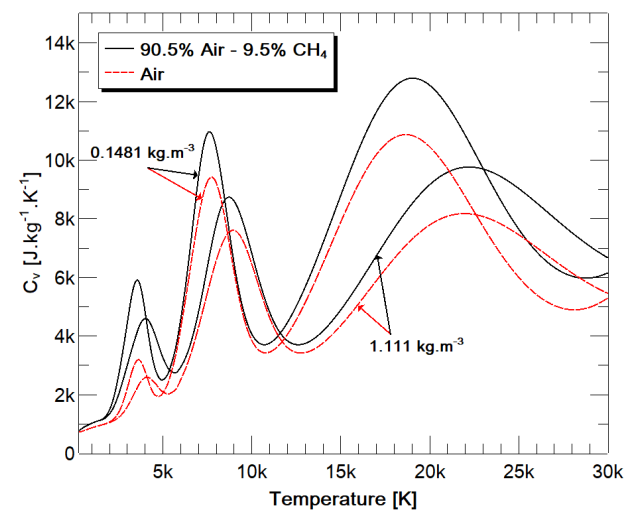
The chemical compositions for a pressure of 1 bar and 10 bars and at a density of 0.1481 kg.m⁻³ and 1.111 kg.m⁻³ are shown respectively in Figure 4 and Figure 5.

At a given pressure (Figure 4), we observe that neutral species dominate the medium at low temperature ($T < 10$ kK). The densities of molecular species gradually decrease with temperature. Then these molecules dissociate to give neutral atoms. The various processes of electron formation, recombination and ionization of species then occur. At high temperatures the ionized species become predominant and neutrals negligible. Increasing pressure changes species behavior. The processes of species transformation are then shifted to higher temperatures. Chemical compositions (Figure 5) with constant density have characteristics similar to those at a given pressure. The species N₂, H₂O and CO₂ are the most predominant at low temperature. As the temperature increases, they are

replaced by neutral atoms, then electrons as well as ionized species. Species densities increase with the value of the mass density. For a given value of mass density, densities of dominant species vary slightly with the temperature. Variations occur only when a given energy is reached (dissociation or ionization temperature) allowing the species to dissociate or ionize according to the type.

3.2. Thermodynamic properties

In Figures 6 and 7 the internal energy and the specific heat at constant volume of the air-methane mixture and air are compared. Figure 6 shows an increasing evolution of internal energy with temperature. Small waves are observed that correspond to the various chemical reactions occurring. The value of internal energy is inversely proportional to the mass density. For the gases compared here, above around 4 kK, the mixture of 90.5% air and 9.5% CH₄ allows a better heat exchange between the system and the external medium compared to pure air because its internal energy is more predominant. With regard to Figure 7 representing specific heat at constant volume, three main peaks, more or less pronounced are present. They correspond to the dissociation of the molecule O₂, then that of N₂, and the ionization of N that we find in the case of air. The peaks that correspond to the different processes move towards higher temperatures with the increase in mass density

Figure 6. Internal energy: 90.5% air and 9.5% CH₄ for 0.1481 and 1.111 kg.m⁻³ at LTE.Figure 7. LTE Specific heat capacity at constant volume: 90.5% air and 9.5% CH₄ for 0.1481 and 1.111 kg.m⁻³ at LTE.

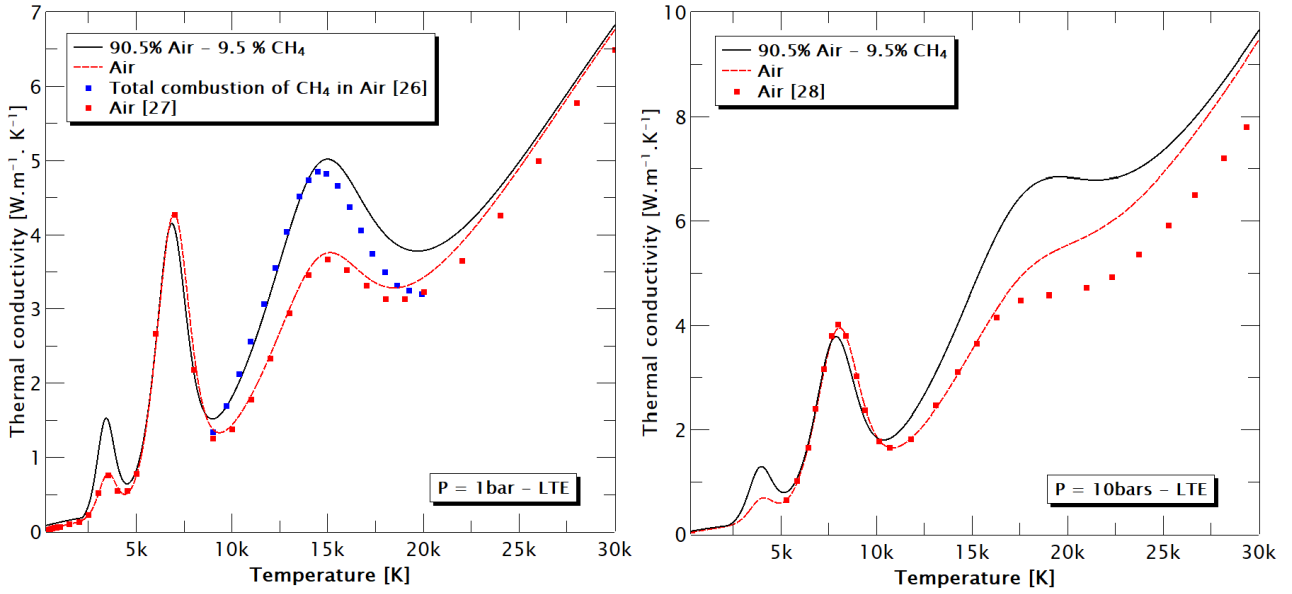


Figure 8. Thermal conductivity: 90.5% air and 9.5% CH_4 and Air for 1 and 10 bars at LTE. Comparison with literature [29–31]

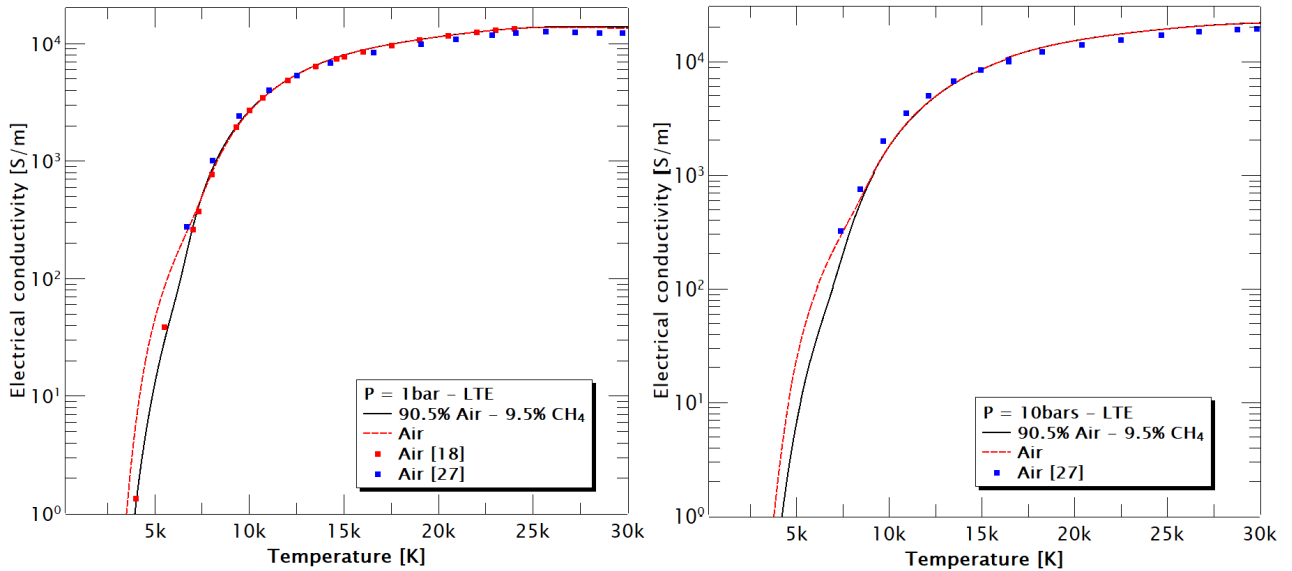


Figure 9. Electrical conductivity: 90.5% air and 9.5% CH_4 and Air for 1 and 10 bars at LTE. Comparison with literature [18, 30]

as we found on chemical compositions (Figure 5). For 9.5% of methane in air, the results show significant differences compared to pure air.

3.3. Transport coefficients

Figures 8, 9 and 10 respectively show the thermal conductivity, the electrical conductivity and the viscosity of 90.5% air and 9.5% CH_4 mixture and the pure air at a pressure of 1 and 10 bars. In order to validate our developments, we compare these data with the available literature results.

Figure 8 describes the evolution of thermal conductivity. They result from the contribution of three terms including internal thermal conductivity, translation and reaction. Below 20 kK, the medium is

dominated mainly by thermal conductivity of reaction, and by small contributions of the internal component as well as the translation of heavy particles. This explains the presence of peaks series similar to the specific heat curves reflecting the chemical reactions that occur. Through the formation of electrons and ionization processes at high-temperature, neutral species begin to disappear. From there, the electron translation component represents an essential part of the total thermal conductivity. We also notice in this case the dependence of the thermal conductivity on the pressure. The peaks also shift to the high temperatures and their amplitudes decrease when the pressure increases. However, when the electronic translation component becomes dominant, the phenomenon re-

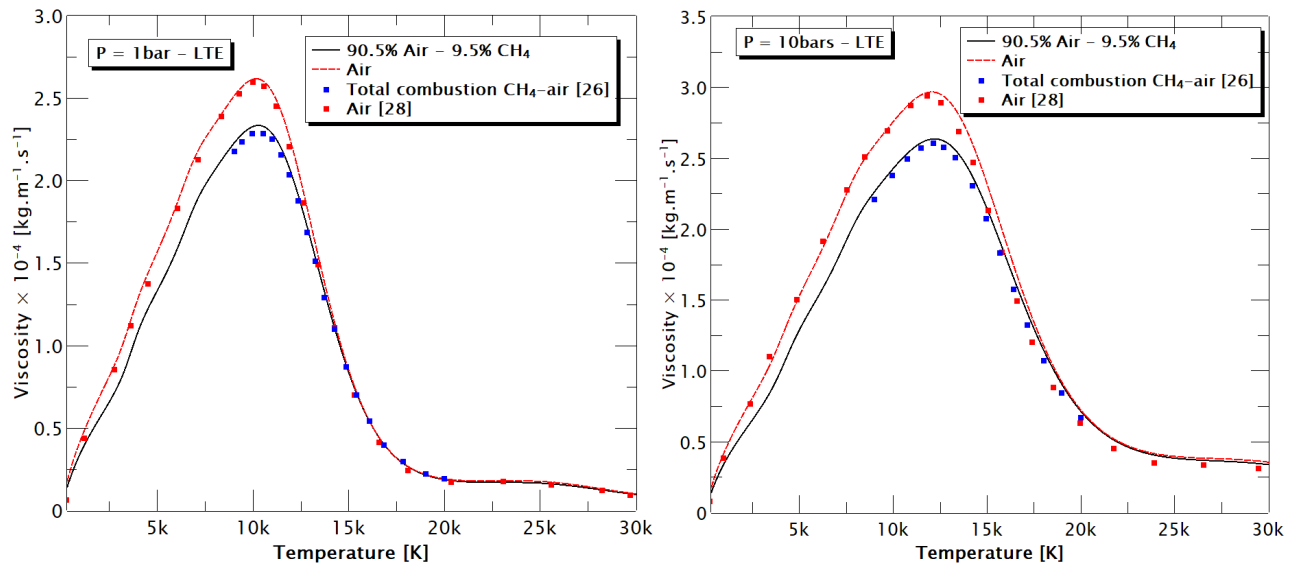


Figure 10. Viscosity : 90.5% air and 9.5% CH₄ and Air for 1 and 10 bars at LTE. Comparison with literature [29, 31]

verses and the thermal conductivity increases with the pressure. In comparison with air, the air-CH₄ mixture allows overall a better ability to drive heat. For electrical conductivity, Figure 9 compares our work with two literature results. There is a strong increase for temperatures up to 10 kK, followed by a quasi-linear variation and finished with a constant profile where the electron density begins to stabilize as can be seen in the case at 1 bar above 25 kK (Figure 9 left). The electrical conductivity depends heavily on the electronic density, the differences observed between the two gases studied are in principle in the region of the strong gradient ($T < 10$ kK). In this area of temperature, electrons vary as a result of ionization phenomena such as molecule NO. In the case of the air-CH₄ mixture, the formation of this molecule results from several species, and as the proportion of air is reduced in the mixture, its quantity in the medium also decreases. As a result, the ionization of NO is delayed compared to that of air, hence a relatively low electronic density.

In Figure 10 the viscosities of 90.5% air and 9.5% CH₄ mixture, as well as the air at a pressure of 1 and 10 bars are confronted with the literature. We find the typical bell shape, with a maximum that reflects the transition from neutral or weakly ionized plasma to a fully ionized medium. As the molar fraction of the species is involved in the viscosity equation, it also depends on the pressure. We then see an increase values and the movement of the maximum toward higher temperatures when the pressure increases. The gap observed between the two gases presented here can be explained by the difference in the values of molar masses and the number of collisions between particles, especially neutrals.

For the transport coefficients compared with the literature presented in this work, we find generally a good agreement. The differences may be due to the

lack of consideration of some species or the choice of collision integrals.

4. Conclusions

The objective of this study was to determine the LTE data for the mixture of 90.5% air and 9.5% CH₄ (chemical composition, thermodynamic properties and transport coefficients). For this purpose, tools have been developed allowing access to these quantities for a large temperature range. We first showed the ability of our developments to calculate the chemical composition for a given pressure or density value. The results illustrate fairly similar behavior of the different species transformation processes between the case at $P = 1$ or 10 bars and at $\rho = 0.1481$ or 1.111 kg.m⁻³. However, for a given mass density, species evolve differently with the particularity of keeping a linear variation up to their respective dissociation or ionization temperatures. We then presented the thermodynamic properties and transport coefficients of the air-CH₄ mixture compared with those of air. For a proportion of 9.5% of CH₄ in air, the results show an important difference in the properties of these two gases. If we want a better prediction of the real plasma behavior in the models, these differences cannot be ignored and the data of 90.5% of air and 9.5% of CH₄ mixture must be used.

Information: The authors can be contacted at the given email to obtain the plasma composition, thermodynamic properties and transport coefficients.

References

- [1] R. Maly and M. Vogel. Initiation and propagation of flame fronts in lean methane/air mixtures by the three modes of the ignition spark. *Int. Symp. on combustion*, 17(1), 1979. doi:10.1016/S0082-0784(79)80079-X.

- [2] V. Kravchik and E. Sher. Numerical modeling of spark ignition and flame initiation in a quiescent methane-air mixture. *J. Combustion and Flame*, 99, 1994. doi:10.1016/0010-2180(94)90057-4.
- [3] C. Zaepffel, D. Hong, and J.-M. Bauchire. Experimental study of an electrical discharge used in reactive media ignition. *J. Phys. D: Appl. Phys.*, 40, 2007. doi:10.1088/0022-3727/40/4/020.
- [4] C. Zaepffel. *Etude expérimentale et numérique d'une décharge électrique appliquée à l'allumage d'un milieu réactif*. PhD thesis, Thèse de doctorat en Physique des gaz et des plasmas, Université d'Orléans, 2008.
- [5] Y. Kramida, A. Ralchenko and J. Reader. NIST atomic spectra database (ver. 5.6.1). URL: <https://physics.nist.gov/asd>.
- [6] M. W. Chase, C. A. Davies, D. J. Downey, J. R. Frurip, R. A. McDonald, and A. N. Syverud. NIST-JANAF thermochemical tables (ver. 1.0). doi:10.18434/T42S31.
- [7] K. S. Drellishak, D. P. Aeschliman, and A. B. Cambel. Partition functions and thermodynamic properties of nitrogen and oxygen plasmas. *Phys. Fluids*, 8(1590), 1965. doi:10.1063/1.1761469.
- [8] M. Capitelli and E. Molinari. Problems of determination of high temperature thermodynamic properties of rare gases with application to mixtures. *Journal of Plasma Physics*, 4(335-550), 1970. doi:10.1017/S0022377800005043.
- [9] G. Colonna, A. D'Angola, and M. Capitelli. Electronic excitation and isentropic coefficients of high temperature planetary atmosphere plasmas. *Physics of Plasmas*, 19(7), 2012. doi:10.1063/1.4737190.
- [10] M. Capitelli, G. Colonna, and A. D'Angola. *Fundamental Aspects of Plasma Chemical Physics: Thermodynamics*. Springer Series on Atomic, Optical, and Plasma Physics, 2013. ISBN 978-1-4419-8182-0.
- [11] A. Harry Solo, P. Freton, and J.-J. Gonzalez. The virial effect – application for SF₆ and CH₄ thermal plasmas. *J. Appl. Sci.*, 9(5), 2019. doi:10.3390/app9050929.
- [12] D. Godin. Calcul de compositions chimiques de plasmas à l'équilibre thermodynamique: application à la modélisation de l'ablation dans les disjoncteurs. Master's thesis, Maitrise en ès sciences appliquées, Université de Montréal – Ecole Polytechnique, Montréal, 1998.
- [13] T. Billoux. *Elaboration d'une base de données radiatives pour des plasmas de type CwHxOyNz et application au transfert radiatif pour des mélanges air, CO₂ et CO-H₂*. PhD thesis, Thèse de doctorat en Ingénierie des Plasmas, Université de Toulouse III - Paul Sabatier, Toulouse, 2013.
- [14] D. Godin and J.-Y. Trepanier. A robust and efficient method for the computation of equilibrium composition in gaseous mixtures. *Plasma Chemistry and Plasma Processing*, 24(3), 2004. doi:10.1007/s11090-004-2279-8.
- [15] A. Harry Solo, P. Freton, and J.-J. Gonzalez. Compositions chimiques et propriétés thermodynamiques à l'échelle d'un mélange air-CH₄. *JITIPEE*, 5(2), 2019. doi:10.18145/jitipee.v5i2.221.
- [16] H. Kallmann. Thermodynamic properties of real gases for use in high pressure problems. Technical report, U.S. Air Force, Project Rand, RM 442, 1950. URL: https://www.rand.org/pubs/research_memoranda/RM442.html.
- [17] C. Wan, Y. Wu, Z. Chen, F. Yang, Y. Feng, M. Rong, and H. Zhang. Thermodynamic and transport properties of real air plasma in wide range of temperature and pressure. *Plasma Science and Technology*, 18(7), 2016. doi:10.1088/1009-0630/18/7/06.
- [18] M. Boulos, P. Fauchais, and E. Pfender. *Thermal Plasmas: Fundamentals and Applications*, volume 1. Springer Science & Business Media, 1994. ISBN 978-1-4899-1339-5.
- [19] P. André, L. Brunet, W. Bussière, J. Caillard, J.-M. Lombard, and J.-P. Picard. Transport coefficients of plasmas consisting of insulator vapours: Application to PE, POM, PMMA, PA66 and PC. *Eur. Phys. J. Appl. Phys.*, 25, 2004. doi:10.1051/epjap:2004007.
- [20] Y. Cressault and A. Gleizes. Thermodynamic properties and transport coefficients in Ar-H₂-Cu plasmas. *J. Phys. D: Appl. Phys.*, 37, 2004. doi:10.1088/0022-3727/37/4/008.
- [21] E. Mason, R. Munn, and F. Smith. Transport coefficient of ionized gases. *Phys. Fluids*, 10(8), 1967. doi:10.1063/1.1762365.
- [22] J. Hirschfelder, C. Curtiss, and R. Bird. *Molecular theory of gases and liquids*. J. Wiley & sons, inc., New York and Chapman & Hal, limited, London, 1954. ISBN 978-0-471-40065-3.
- [23] M. Capitelli, C. Gorse, S. Longo, and D. Giordano. Collision integrals of high temperature air species. *J. Thermophysics and Heat Transfer*, 14(2), 2000. doi:10.2514/2.6517.
- [24] J.-M. Baronnet, A. Sanon, B. Sauvage, J. Lesinski, E. Meillot, and G. Debbagh-Nour. Transport coefficient of hydrogen-methane thermal plasma. In *8th International Symposium on Plasma Chemistry, Symposium Proceedings*, page p125, 1987. URL: <https://www.ispc-conference.org/ispcdocs/ispc8/DB2.html>.
- [25] A. Sanon. *Contribution au calcul des propriétés thermodynamiques et des coefficients de transport de plasmas thermiques de mélanges Ar-H*. PhD thesis, Thèse de doctorat en physique, Université de Limoge, France, 1988.

- [26] A. Sanon. Transport coefficients of Ar-C-H-O-N systems thermal plasma at atmospheric pressure. *IOP Conf. Ser.: Mater. Sci. Eng.*, 2012. doi:10.1088/1757-899X/29/1/012003.
- [27] A. D'Angola, G. Colonna, A. Bonomo, D. Bruno, A. Laricchiuta, and M. Capitelli. A phenomenological approach for the transport properties of air plasmas. *The European Physical Journal D*, 66, 2012. doi:10.1140/epjd/e2012-30147-8.
- [28] M. Capitelli, C. Gorse, S. Longo, and D. Giordano. Collision integrals of high-temperature air species. *J. Thermophys. and Heat Transfer*, 14(2), 2000. doi:10.2514/2.6517.
- [29] B. Sourd, J. Aubreton, M.-F. Elchinger, M. Labrot, and U. Michon. High temperature transport coefficients in e-C-H-N-O mixtures. *J. Phys. D: Appl. Phys.*, 39, 2006. doi:10.1088/0022-3727/39/6/016.
- [30] M. Capitelli, G. Colonna, C. Gorse, and A. d'Angola. Transport properties of high temperature air in local thermodynamic equilibrium. *Eur. Phys. J. D.*, 11, 2000. doi:10.1007/s100530070094.
- [31] A. D'Angola, G. Colonna, C. Gorse, and M. Capitelli. Thermodynamic and transport properties in equilibrium air plasmas in a wide pressure and temperature range. *Eur. Phys. J. D.*, 46, 2008. doi:10.1140/epjd/e2007-00305-4.